

# Hydrogen Production via Catalytic Decomposition of Methane

T. V. Choudhary, C. Sivadinarayana, C. C. Chusuei, A. Klinghoffer, and D. W. Goodman<sup>1</sup>

*Department of Chemistry, Texas A&M University, College Station, Texas 77842*

Received June 12, 2000; revised December 6, 2000; accepted December 6, 2000; published online February 26, 2001

Methane decomposition on various Ni-supported catalysts has been investigated as a method for production of CO-free hydrogen for use in fuel cells. The low levels of CO formed due to the interaction of surface carbon (formed from methane decomposition) with the support have been quantitatively analyzed (part per million levels) by methanation of the CO and subsequent analysis by flame ionization detection (FID). This study highlights the dependence of the type of carbon formed and the amount of CO evolved on the nature of the support. No filamentous carbon was observed on Ni/H-ZSM-5 at elevated methane decomposition temperatures, whereas Ni/HY and Ni/SiO<sub>2</sub> showed filamentous carbon formation over the entire temperature range studied (723 K to 873 K). While two forms of carbon (carbide and graphitic) were observed on the Ni/SiO<sub>2</sub> after methane decomposition at 723 K, only graphitic carbon was observed at 823 K. The rate of CO formation was observed to be highest on Ni/H-ZSM-5 and lowest on Ni/SiO<sub>2</sub>. The CO formation rates showed a common trend for all the catalysts: high initial rates followed by a lower stabilized rate. The CO formation rates were found to increase with increasing temperature. The CO content in the hydrogen stream was ca. 50 ppm and 250 ppm for Ni/SiO<sub>2</sub> and Ni/HY, respectively, after the CO production rates stabilized. The low levels of CO coupled with the stability of the catalysts for methane decomposition make this an interesting conceptual process for hydrogen production for fuel cell applications. Regeneration studies have shown that there is no loss of activity for methane decomposition at 723 K on Ni/H-ZSM-5 over many reaction cycles. © 2001 Academic Press

**Key Words:** step-wise reforming; methane decomposition; CO-free hydrogen; filamentous carbon.

## INTRODUCTION

Fuel cells being environmentally benign and highly efficient represent an exciting form of technology for converting the chemical energy of a fuel directly into electricity. Methane (the main constituent of natural gas), due to its large abundance and high C/H ratio, is an ideal source of hydrogen (which is the best known primary fuel for fuel cells). Phosphoric acid fuel cells, which are the most commercially developed fuel cells, do not tolerate CO concentrations above 1.5%. The CO-free requirement of the hydrogen

stream is even more stringent (ppm level) for the more recently developed proton exchange membrane (PEM) fuel cells. Conventional processes such as steam reforming of methane, partial oxidation, and autothermal reforming (1–4) produce significant amounts of CO along with hydrogen. Removal of CO from the hydrogen stream not only increases the complexity but also is highly detrimental to the total process economics. It is therefore of interest to explore other alternatives for the production of CO-free hydrogen.

Decomposition of methane has been studied quite extensively for methane homologation reactions (5–8) and fundamental dynamical studies (9, 10); however, methane decomposition as a method to obtain pure hydrogen has received relatively little attention (11, 12). We have recently proposed stepwise steam reforming of methane to produce CO-free hydrogen (13, 14). This process, which operates at relatively low temperatures ( $\leq 673$  K), involves the catalytic decomposition of methane in a first step to produce CO-free hydrogen and surface carbon and/or hydrocarbonaceous species followed by a separate step in which the surface carbon/carbonaceous species is removed via reaction with water. However, the methane conversions are small at low temperatures; hence, it is important to investigate conversions at higher temperatures.

It has been shown that at temperatures above 823 K, Ni-based catalysts exhibit stable operation for a few hours, providing 2 mol of hydrogen per mole of methane reacted (12). Methane decomposition can result in carbon yields as high as 384 g<sub>C</sub>/g<sub>Ni</sub> on 90% Ni/SiO<sub>2</sub> in a vibro-fluidized catalyst bed at 823 K (15, 16). The absence of rapid catalytic deactivation is explained by the diffusion of carbonaceous species into the bulk of the metal particles. The latter process generates active surface sites for dehydrogenation of subsequent methane molecules resulting in the formation of filamentous carbon. Recently, it has been noted that decomposition of methane may lead to CO formation via reaction of the carbonaceous residue with the oxygen of the oxide support (17). These studies, however, did not provide CO and hydrogen formation rates under steady state conditions and hence the CO content in the hydrogen stream could not be determined. The CO issue is currently the most crucial aspect in fuel processing for fuel cells. Since

<sup>1</sup> To whom correspondence should be addressed. Fax: (979) 845-6822. E-mail: [goodman@mail.chem.tamu.edu](mailto:goodman@mail.chem.tamu.edu).



the main advantage offered by the stepwise reforming process is production of hydrogen with extremely low levels of CO, accurate analysis of this CO content in the product stream and study of factors influencing the CO content become imperative. To address this issue, in this work efforts have been undertaken to monitor extremely small concentration of CO (ppm levels could be analyzed employing a methanizer coupled with a flame ionization detector). The influences of the support and reaction conditions on the CO content have been investigated in this work. Transmission electron microscopy (TEM) and X-ray photoelectron spectroscopy (XPS) were employed to study the nature of the surface carbon; CO pulse experiments were carried out to measure the specific metal surface area.

## EXPERIMENTAL

### a. Catalyst Synthesis

Ni catalysts supported on H-ZSM-5, HY, and SiO<sub>2</sub> were synthesized by conventional wet-impregnation with a nominal metal loading of 10 wt%. Ni(NO<sub>3</sub>)<sub>2</sub>·6H<sub>2</sub>O (amount corresponding to 10 wt% Ni in the catalyst was used for impregnation) salt was used as the source of Ni metal and in each case the impregnation procedure was performed at room temperature. H-ZSM-5 (Code No. DAZ-P; Si/Al = 500; surface area, 400 m<sup>2</sup>/g; and pore volume, 0.18 cm<sup>3</sup>/g) and NaY (Code No. DAY-P; Si/Al = 100; surface area, 700 m<sup>2</sup>/g; and pore volume, 0.3 cm<sup>3</sup>/g) were obtained from Degussa and SiO<sub>2</sub> (Cab-O-Sil; surface area, 325 m<sup>2</sup>/g; and surface density of hydroxyl groups, 3.055 nm<sup>-2</sup>) was obtained from Cabot Corp. NaY was converted to HY via aqueous ion exchange (ammonium hydroxide solution). The procedure was repeated 3–6 times to achieve a high degree of ion exchange. Prior to loading Ni on silica, the silica was calcined overnight at 823 K. After impregnation, the catalysts were dried overnight at ~373 K and then calcined at 823 K for 4 h. The powder catalysts were then pressed, crushed, and sieved to a 20–40 mesh size.

### b. Apparatus and Analytical Techniques

The continuous-flow reactor system consisted of a conventional fixed-bed plug-flow stainless steel (SS) reactor and a furnace controlled by a temperature controller. The SS reactor was 10 in. long with  $\frac{3}{8}$  in. O.D. with a small section serving as the catalyst bed. The analysis system consisted of a thermal conductivity detector (TCD), a flame ionization detector (FID), and a methanizer. The gases to be analyzed first passed through the TCD and finally reached the FID via the methanizer (Carle Cat. No. 0117). The FID was calibrated over a large dynamic range for methane. Essentially 100% conversion efficiency (CO to methane) was achieved by operating the methanizer at 400°C with large amounts of hydrogen. This was accomplished by routing

all of the hydrogen flow to the FID through the methanizer. An auxiliary flow of carrier gas was employed to obtain the optimum carrier/hydrogen ratio for maximum detector sensitivity. Various amounts of CO were injected into the methanizer to check for 100% conversion of CO to methane. This process was repeated regularly to ensure complete conversion of CO. If any aberration was observed the methanizer was regenerated (oxidation followed by reduction) until quantitative conversion of CO to methane was observed. Regular regeneration/testing of the methanizer assured constant reproducible complete conversion of CO to methane.

Before the reaction, the catalyst was reduced with H<sub>2</sub> in flowing Ar at a total flow rate of 20 ml/min for 0.5 h at 523 K and at 723 K for 2.5 h at 723 K. Following this, the catalyst was flushed with Ar for 0.5 h and heated to the desired reaction temperature in a flow of carrier gas. High purity gases (20% CH<sub>4</sub> in Ar (certified mixture), Ar (UHP), hydrogen (zero grade), and air (zero grade)) were employed for this investigation. Product analysis showed that 2 mol of hydrogen per mole of methane consumed were formed for all the catalysts and conditions investigated. Though small amounts of CO<sub>2</sub> (<500 ppm) were sometimes observed, no emphasis was placed on CO<sub>2</sub> analysis as CO<sub>2</sub> does not pose serious problems in the operation of acid fuel cells. The catalyst was weighed before and after the methane decomposition reactions and a carbon mass balance of ±5% was obtained.

### c. Catalyst Characterization

1. *X-ray photoelectron spectroscopy.* XPS was performed in an ion-pumped (300 L/s) Perkin-Elmer PHI 560 system using a PHI 25-270AR double-pass cylindrical mirror analyzer. A Mg K $\alpha$  anode with a photon energy of 1253.6 eV was operated at 15 kV and 300 W. Survey scans were performed using a 100 eV pass energy; high-resolution scans were performed with a 50 eV pass energy. Core levels of the C(1s), O(1s), Al(2p), Al(2s), Si(2p), and Ni(2p) orbitals were scanned and normalized to their respective atomic sensitivity factors (18). The system pressure during XPS analysis was  $\sim 1 \times 10^{-8}$  Torr. The Cu(2p<sub>3/2</sub>), (932.7 eV) and Au(4f<sub>7/2</sub>) (84.0 eV) orbitals were used as standards from sputter-cleaned foils to calibrate the XPS BE range (19). The precision of the BE measurements was ±0.2 eV. Signal from adventitious carbon at BE = 284.7 eV for the C(1s) level was used to correct for sample charging (20). Samples were mounted onto a 1.0 cm × 1.0 cm × 1.0 cm support using double-sided tape (Scotch, 3M) attached to a probe and introduced into the UHV via a turbo-pumped antechamber. The support was attached to a probe that was differentially pumped using sliding seals. Curve fitting of the XPS data was performed using Peakfit ver. 3.1 B (Jandel Scientific) software.

2. *Specific area measurements.* The Ni surface area was measured by CO pulse adsorption experiments carried out at room temperature assuming a CO/Ni ratio of 1.0. Prior to the Ni surface area determination, the catalyst was pre-reduced for 0.5 h at 523 K and for 2.5 h at 723 K in flowing H<sub>2</sub> and He, and then brought to room temperature in flowing He. The analysis of CO was carried out online with a TCD.

3. *TEM characterization.* TEM micrographs of the supported Ni catalysts were obtained using a high-resolution Jeol 2010 instrument (Electron Microscopy Center, Texas A&M University). Samples after reaction were ultrasonically dispersed in acetone and spread over perforated molybdenum grids. Several bright-field TEM micrographs of different portions of the sample were obtained at magnifications up to 400,000.

4. *Diffuse reflectance infrared spectroscopy (DRIFTS).* The DRIFTS experiments were performed with a Perkin-Elmer Spectrum 2000 spectrometer equipped with an MCT detector and a DRIFTS (Harrick) cell used in a flow mode. Mixtures of silica (10 % Ni/SiO<sub>2</sub>) and KBr (ratio of 1 : 7) were packed in a metal cup reactor whose temperature could be varied from ambient to 873 K. The cell was purged with dry nitrogen for at least 4 h prior to the DRIFTS experiment. The DRIFTS spectrum of SiO<sub>2</sub> (same batch that was used for preparing the Ni/SiO<sub>2</sub> catalyst) was obtained after heating the sample to 373 K for 1 h under flow of He to remove the adsorbed water. Prior to obtaining the spectra on the Ni/SiO<sub>2</sub> catalyst, it was pretreated in the same manner as in the conventional catalytic reactor and heated to the reaction temperature of 823 K.

## RESULTS AND DISCUSSION

### a. Surface Characterization

1. *CO pulse experiments.* The results obtained from CO pulse experiments are shown in Table 1. Metal dispersions have been calculated from the CO uptake assuming an adsorption stoichiometry of one CO molecule per Ni site. The metal loading was the same for all the catalysts studied (10 wt% Ni). The highest catalyst dispersion was observed on H-ZSM-5 support and the lowest on HY. The measured specific area for all the catalysts was less than

TABLE 1

CO Chemisorption Data on Ni-Supported Catalysts

Catalyst	CO adsorbed ( $\mu\text{mol g}^{-1}$ )	Dispersion (%)	Particle size <sup>a</sup> (nm)
10% Ni/H-ZSM-5	52	3.1	32
10% Ni/HY	7	0.4	250
10% Ni/SiO <sub>2</sub>	16	1.0	100

<sup>a</sup> From chemisorption data.

5 m<sup>2</sup>/g. The average particle size ranged from 30–250 nm for the catalysts under consideration and was measured from the chemisorption data using the usual approximation (21): (a) metal particles have a spherical geometry and (b) surface is formed from equal proportions of the main low-index planes.

2. *TEM and XPS.* Figure 1a shows the TEM micrograph of Ni/H-ZSM-5 catalyst after interaction with methane and complete deactivation at 723 K. The figure shows a single crystal of H-ZSM-5 with carbon filaments projecting from it. Such outgrowths of filamentous carbon from the sides of the H-ZSM-5 were observed throughout the sample. Figure 1b shows the image of a single filament of carbon. The pear-shaped Ni particle is present at the apex of the filament. Growth of filamentous carbon involves the adsorption and decomposition of methane on various faces of the Ni particle followed by dissolution of some of the carbon species into the bulk and subsequent diffusion through the metal particle due to a concentration gradient (22–24).

No filamentous carbon was observed after the methane decomposition was carried out on Ni/H-ZSM-5 at 973 K instead, TEM micrographs indicate the presence of graphitic carbon, which encapsulates the Ni particles (Fig. 2). In the case of Ni supported on HY and SiO<sub>2</sub>, filamentous carbon formation was observed over the entire temperature range (723 K to 873 K). Figure 3 shows the presence of filamentous carbon on the Ni/HY sample after complete deactivation due to methane decomposition at 823 K. This representative TEM image indicates that the catalyst can support large amounts of filamentous carbon. It is noteworthy that the amount of filamentous carbon formed on Ni/SiO<sub>2</sub> was greater than that on Ni/H-ZSM-5 at 723 K. This suggests that some species other than filamentous carbon were also formed on Ni/H-ZSM-5. Further discussion on this topic will be continued in the XPS section.

Figure 4 shows XP spectra obtained for the C(1s) level after complete deactivation of the Ni/SiO<sub>2</sub> as a result of carbon deposition from methane decomposition reaction at 823 and 723 K, respectively. While a single peak (graphitic carbon) was observed for the higher temperature conditions, two features separated by 2.8 eV were observed after the lower temperature reaction. The graphitic form of carbon (284.7 eV) was assigned to filamentous carbon (as seen in TEM), whereas the lower binding energy peak at 281.9 eV was assigned to carbidic carbon. This assignment is in good agreement with previous XPS literature involving carbide features (25, 26). The presence of the single graphitic peak at 823 K indicates that the carbidic form does not exist at higher temperatures, which is consistent with a previous study (27).

### b. Interaction of Methane with Ni/ZSM-5

Figure 5 shows the total amount of hydrogen (in monolayer equivalents, MLE) produced until complete catalyst

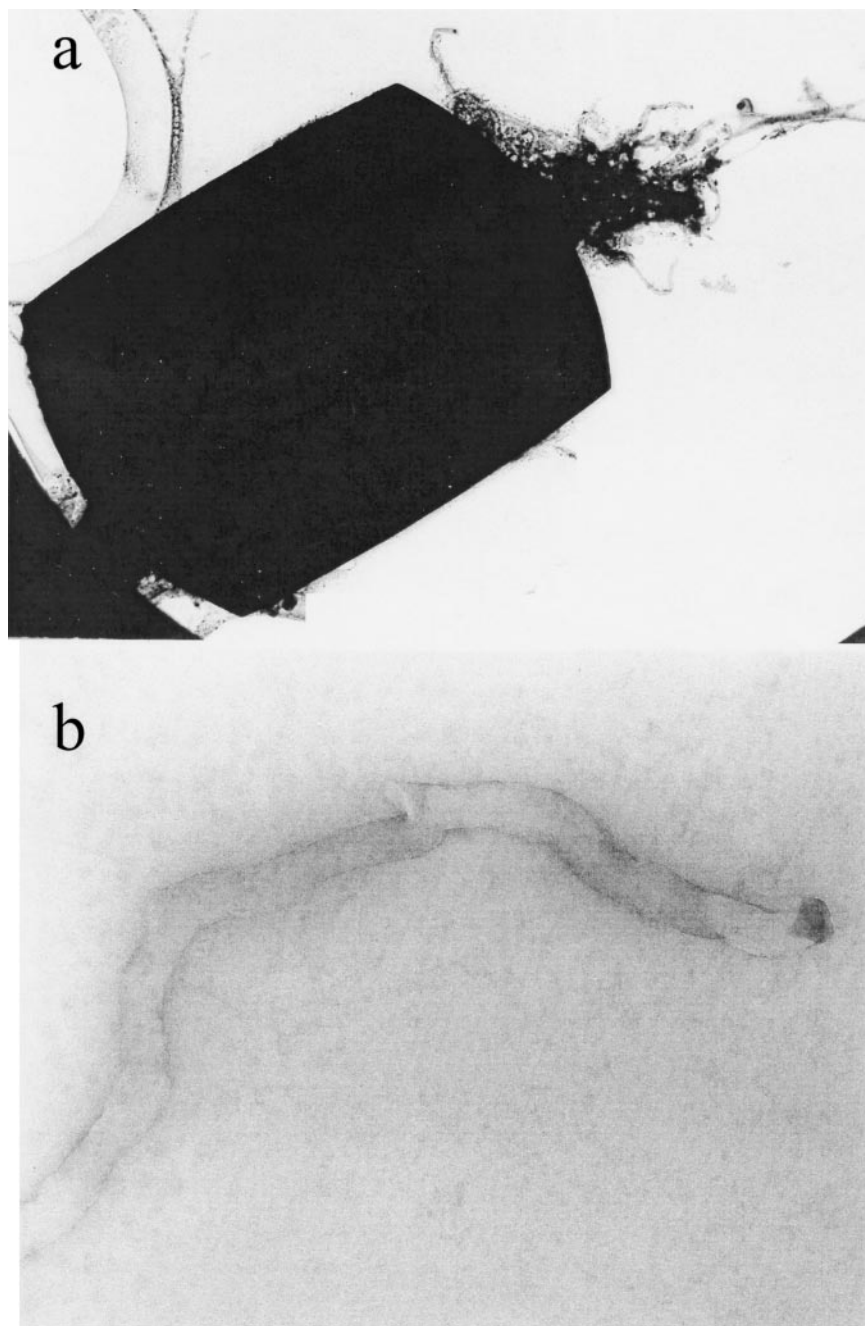


FIG. 1. TEM image of (a) filamentous carbon formed on Ni/H-ZSM-5 and (b) a single filament of carbon at 723 K.

deactivation as a function of reaction temperature on 10% Ni/H-ZSM-5 ( $\text{GHSV} : 15,000 \text{ cm}^3 \cdot \text{g}^{-1} \cdot \text{h}^{-1}$ ). The hydrogen monolayer equivalents (MLE) were estimated from the specific metal surface area assuming one hydrogen monolayer to correspond to a  $C/\text{Ni}_{\text{surface}}$  ratio of 0.5. The total amount of hydrogen produced decreased drastically with increase in reaction temperature. As seen earlier in TEM (Fig. 1a) there was evidence for filamentous carbon formation at 723 K whereas only the encapsulating graphitic type is observed at 973 K. Ni particles, which had been present

during filamentous carbon growth, were available for further methane decomposition and resulted in a greater lifespan of the catalyst. Encapsulation of Ni particles caused rapid deactivation of catalyst and hence the total amount of hydrogen produced is extremely small at 973 K. As the catalyst was fairly stable in the temperature range of 723 to 773 K CO analysis experiments were performed at 723 and 773 K. Figure 6 shows the rate of hydrogen and CO production as a function of time for the two temperatures. As can be seen from the figure, no induction period

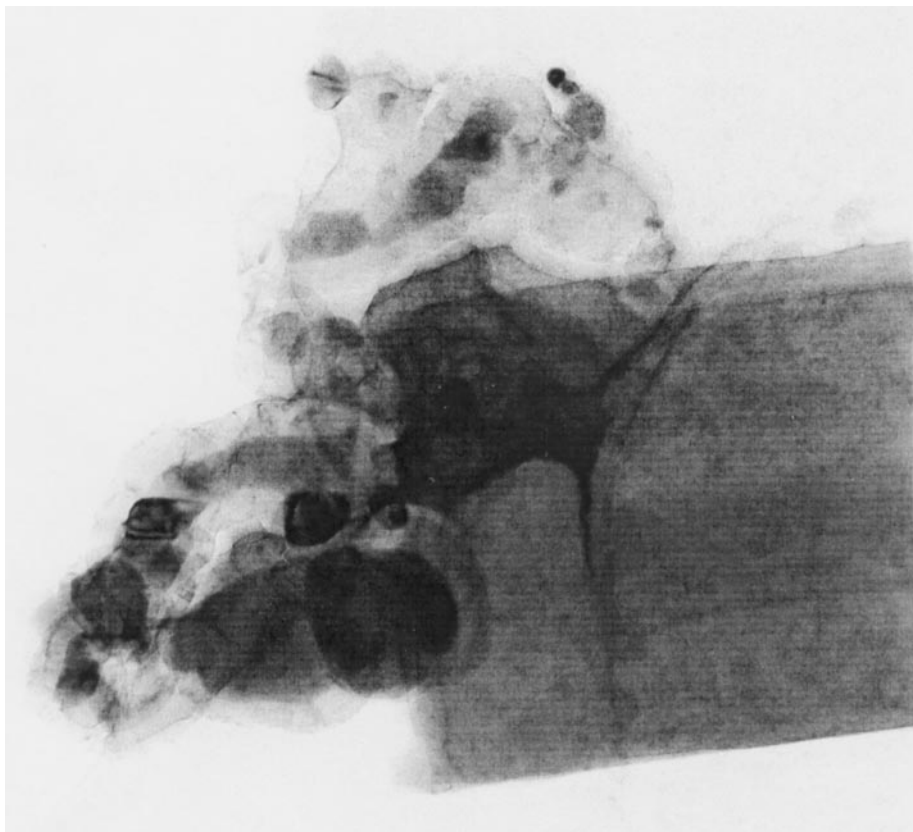


FIG. 2. TEM micrograph of carbon formed on Ni/H-ZSM-5 at 973 K.

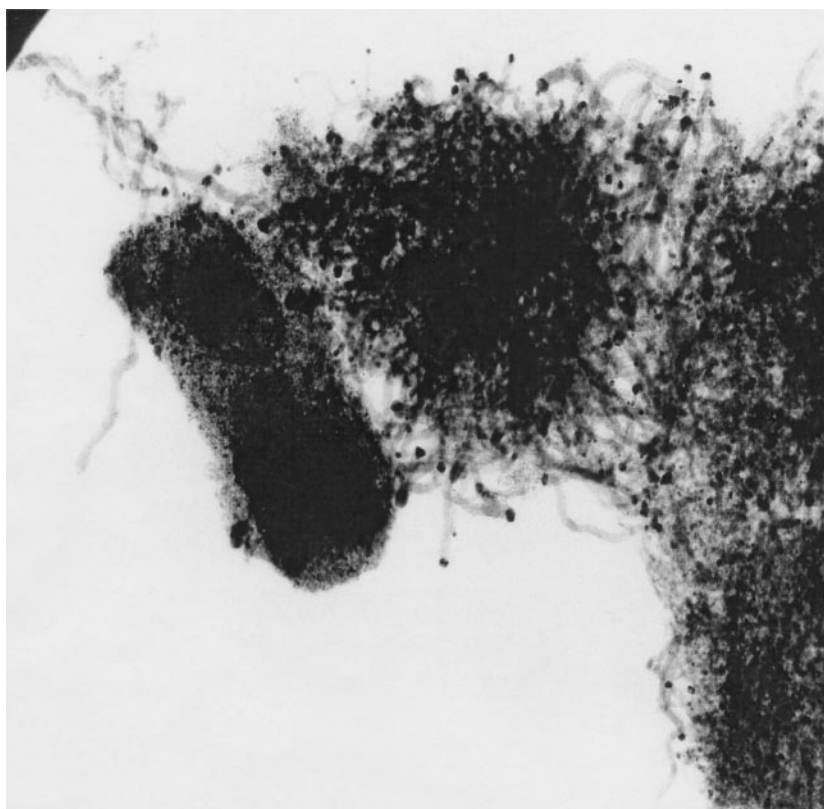


FIG. 3. TEM image of carbon filaments on Ni/HY after methane decomposition reaction at 823 K.

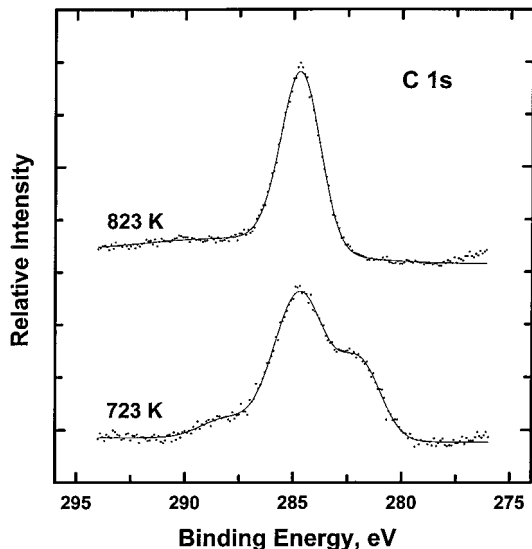


FIG. 4. XPS spectrum of C(1s) formed on Ni/SiO<sub>2</sub> surface after reaction with methane at 723 and 823 K.

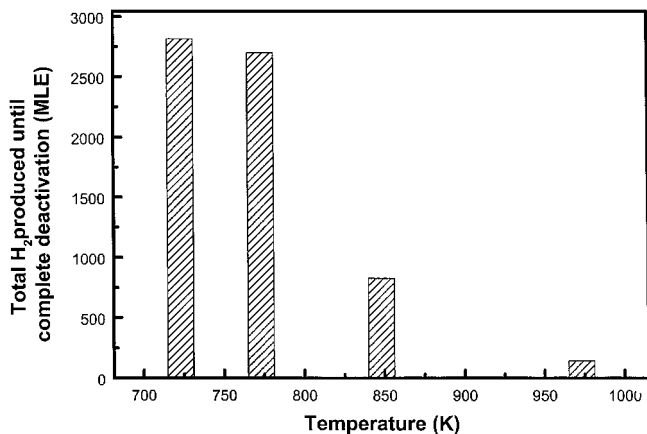


FIG. 5. Effect of temperature on the production of total hydrogen (MLE) on Ni/H-ZSM-5 (GHSV = 150,000 cm<sup>3</sup> · g<sup>-1</sup> · h<sup>-1</sup>; 0.1 g of catalyst).

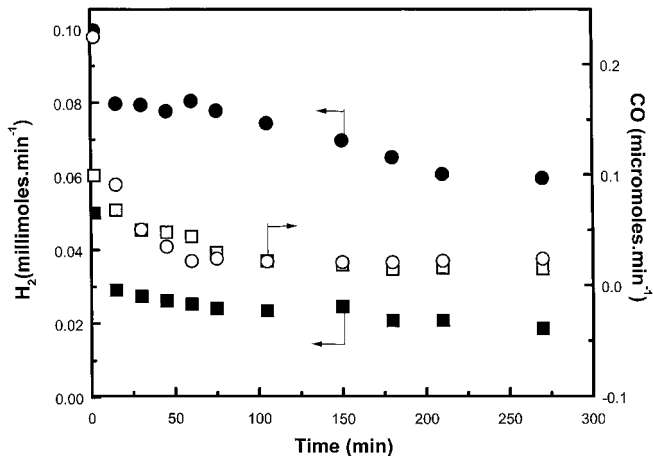


FIG. 6. Time-on-stream data of hydrogen and carbon monoxide formation during methane decomposition on Ni/H-ZSM-5 at 723 K (□, ■) and 773 K (○, ●) (GHSV = 15,000 cm<sup>3</sup> · g<sup>-1</sup> · h<sup>-1</sup>; 0.1 g of catalyst).

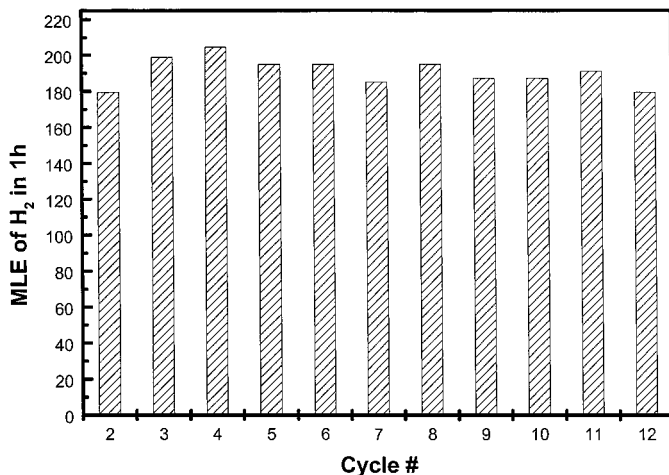


FIG. 7. Hydrogen production on Ni/H-ZSM-5 as a function of regeneration cycles at 723 K (GHSV = 15,000 cm<sup>3</sup> · g<sup>-1</sup> · h<sup>-1</sup>; 0.1 g of catalyst).

(methane conversion did not pass through a maximum) was observed and the rate of hydrogen production at 773 K was more than twice that at 723 K. The initial CO production rate was greater at 773 K, but gradually became comparable with time for both temperatures. Figure 7 shows the data obtained for regeneration cycles on 10% Ni/ZSM-5 at a reaction temperature of 723 K. The following procedure was used for the study: reaction with 20% methane in Ar (60 min at 723 K) followed by regeneration in air (30 min at 723 K) and reduction with 1 : 1 H<sub>2</sub> (15 min at 523 K and 30 min at 723 K). The catalyst was flushed with argon for 30 min before and after the reduction treatment. The figure clearly shows that there was no drop in activity of the catalyst through the 12 cycles studied. A similar study was carried out at a reaction temperature of 773 K (the regeneration with air was carried out at 773 K instead of 723 K); however, in this case a gradual decrease in activity was observed with every cycle (Fig. 8) which we attribute to

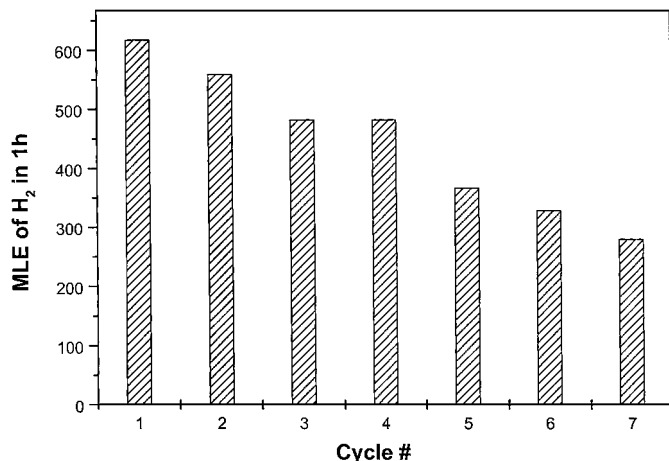


FIG. 8. Hydrogen production on Ni/H-ZSM-5 as a function of regeneration cycles at 773 K (GHSV = 15,000 cm<sup>3</sup> · g<sup>-1</sup> · h<sup>-1</sup>; 0.1 g of catalyst).

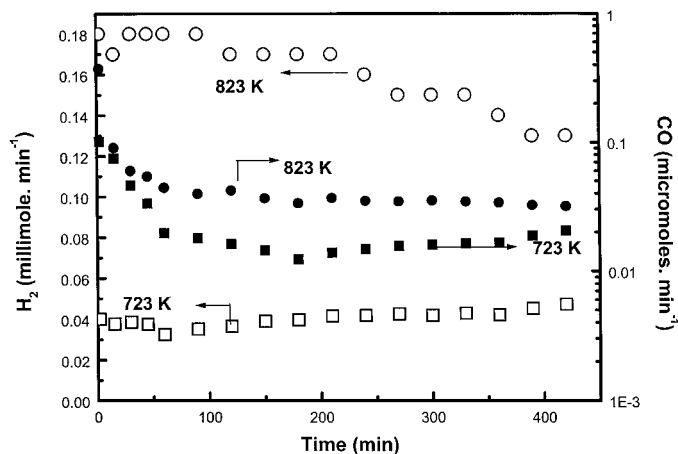


FIG. 9. Time-on-stream data of hydrogen and carbon monoxide formation during methane decomposition on Ni/HY at 723 and 823 K (GHSV =  $20,000 \text{ cm}^3 \cdot \text{g}^{-1} \cdot \text{h}^{-1}$ ; 0.1 g of catalyst).

sintering of the Ni particles at higher temperature (during regeneration).

### c. Methane Decomposition on Ni/HY and Ni/SiO<sub>2</sub>

1. *Ni/HY*. Figure 9 shows the rate of hydrogen and CO production as a function of time during methane decomposition on 10% Ni/HY at 723 K and 823 K (GHSV =  $20,000 \text{ cm}^3 \cdot \text{g}^{-1} \cdot \text{h}^{-1}$ ). Similar to the Ni/ZSM-5 system no induction period is observed. The rate of CO production is higher at 823 K as compared to the rate at 723 K, but due to much larger hydrogen formation rates at 823 K the levels of CO in the hydrogen stream are larger at 723 K. Figure 10 shows the time-on-stream plot for the methane decomposition reaction at 823 K until deactivation. The catalyst, having an initial conversion of 31%, gradually deactivates in

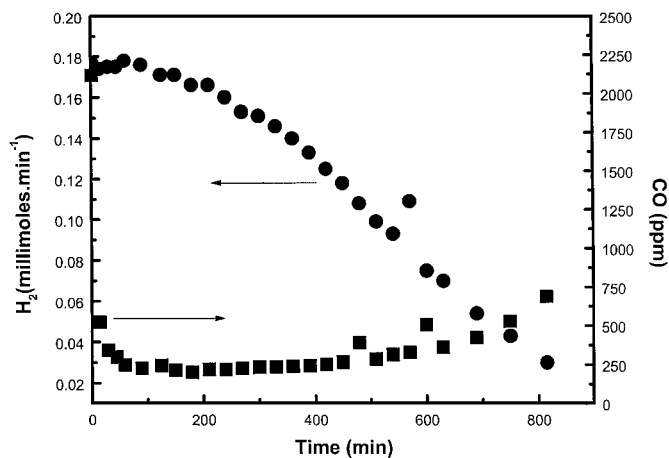


FIG. 10. Total CO content and hydrogen production rates as a function of time for Ni/HY at 823 K (GHSV =  $20,000 \text{ cm}^3 \cdot \text{g}^{-1} \cdot \text{h}^{-1}$ ; 0.1 g of catalyst).

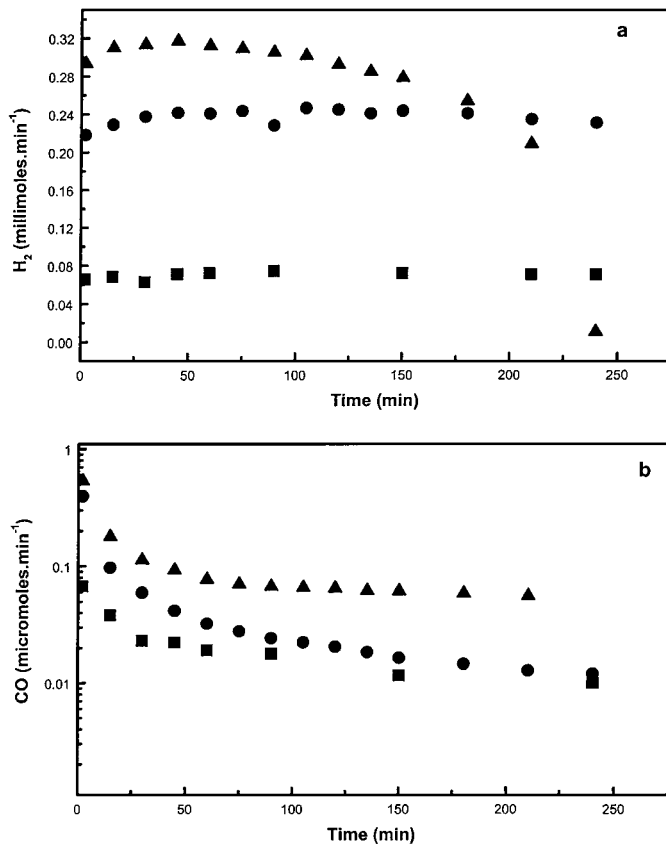


FIG. 11. Time-on-stream data of (a) hydrogen and (b) carbon monoxide formation during methane decomposition on Ni/SiO<sub>2</sub> at 723, 823, and 873 K (GHSV =  $20,000 \text{ cm}^3 \cdot \text{g}^{-1} \cdot \text{h}^{-1}$ ; 0.1 g of catalyst).

ca. 14 h. The amount of CO in the hydrogen stream is high initially (0.2%) but then decreases to ca. 250 ppm (where it stabilizes for  $\sim 8$  h) and finally increases slightly toward the end of the reaction. This increase toward the end can be attributed to the decrease in the rate of hydrogen formation as the catalyst approaches its complete deactivation.

2. *Methane decomposition on Ni/SiO<sub>2</sub>*. Hydrogen and CO formation rates on 10% Ni/SiO<sub>2</sub> at various reaction temperatures are shown in Figs. 11a and 11b, respectively. The rates of hydrogen production on our catalyst (ca. 1.4 mol (H<sub>2</sub>)/g<sub>Ni</sub> h) were found to be comparable with previous methane decomposition studies on Ni/SiO<sub>2</sub> catalysts (ca. 1.1 mol (H<sub>2</sub>)/g<sub>Ni</sub> h (12), ca. 1.7 mol (H<sub>2</sub>)/g<sub>Ni</sub> h (16)) at 823 K. The initial conversion (20% CH<sub>4</sub> in Ar) ranges from 11% at 723 K to 52% at 873 K. Unlike the Ni/H-ZSM-5 and Ni/HY systems, a modest induction period is observed in case of the Ni/SiO<sub>2</sub> catalyst. For the 873 K reaction, rapid deactivation is observed after ca. 4 h, whereas the catalyst shows stable activity for periods much longer than 4 h for the reactions carried out at 723 and 823 K. The total amount of hydrogen produced was found to be larger at 823 than at 873 K. The rate of CO formation on Ni/SiO<sub>2</sub> followed the

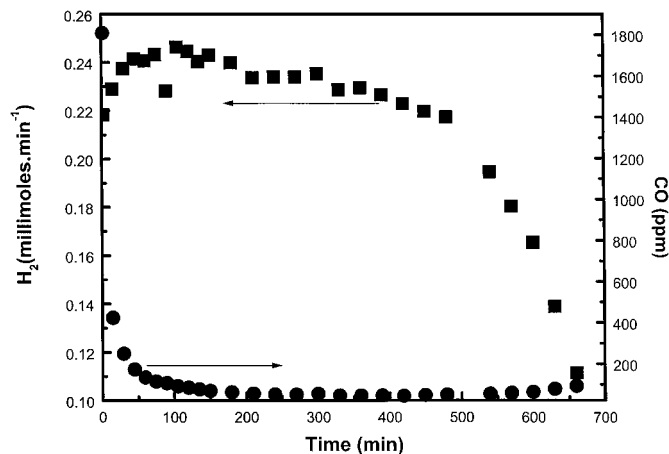


FIG. 12. Total CO content and hydrogen production rates as a function of time for Ni/SiO<sub>2</sub> at 823 K (GHSV = 20,000 cm<sup>3</sup> · g<sup>-1</sup> · h<sup>-1</sup>; 0.1 g of catalyst).

same trends as for the Ni/HY and Ni/ZSM-5 (i.e., rate of CO formation increased with increasing reaction temperatures). Interestingly, the increase in the CO formation rate was greater from 823 to 873 K than from 723 to 823 K. This may be explained by the fact that high temperatures thermodynamically favor CO formation. Figure 12 shows the rate of hydrogen formation and CO content in the hydrogen stream for methane decomposition reaction on Ni/SiO<sub>2</sub> at 823 K (GHSV = 20,000 cm<sup>3</sup> · g<sup>-1</sup> · h<sup>-1</sup>). The catalyst shows stable activity for methane decomposition for ~8 h, and then rapid deactivation. The CO concentration is ~0.2% initially, drops below 100 ppm in 90 min, and then remains at ca. 50 ppm for 6 h after, followed by a slight increase during the deactivation stage of the catalyst. Approximately 1 mol of hydrogen can be produced per gram of catalyst with CO levels close to 50 ppm. Investigations are currently being directed toward decreasing the time required to obtain low levels of CO in the product stream.

#### d. Methane Decomposition: Comparison of Supports

The conversion levels for methane are shown in Fig. 13 as a function of time for the various catalysts studied at 823 K (GHSV = 20,000 cm<sup>3</sup> · h<sup>-1</sup> · g<sup>-1</sup>). The initial methane conversions are comparable for all three catalysts. Complete deactivation is observed for Ni/ZSM-5 in ca. 1 h whereas Ni/SiO<sub>2</sub> and Ni/HY exhibit catalytic activity for methane decomposition in excess of 12 h. As discussed earlier, at high temperatures the graphitic carbon formed on Ni/H-ZSM-5 system encapsulates the Ni particles and leads to rapid deactivation. But in the cases of Ni/HY and Ni/SiO<sub>2</sub>, there is evidence for filamentous carbon formation leading to a longer lifetime of the catalyst. A notable difference observed between the deactivation profiles of Ni/SiO<sub>2</sub> and Ni/HY is that Ni/SiO<sub>2</sub> shows stable activity for ca. 8 h and then deactivates rapidly, whereas for Ni/HY

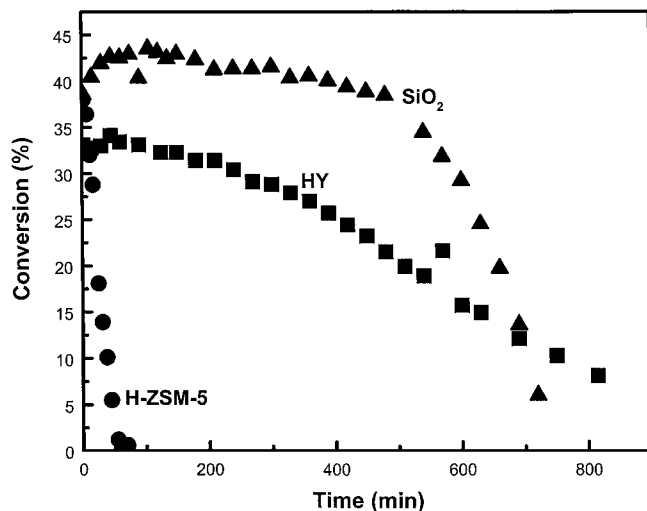


FIG. 13. Comparison of methane conversion as a function of time for Ni supported on HZSM-5, HY, and SiO<sub>2</sub> at 823 K (GHSV = 20,000 cm<sup>3</sup> · g<sup>-1</sup> · h<sup>-1</sup>; 0.1 g of catalyst).

a gradual deactivation is observed. No induction period is observed in the case of Ni/H-ZSM-5 and Ni/HY, whereas Ni/SiO<sub>2</sub> shows an induction period. Figure 14 shows the time-on-stream CO content (in the hydrogen stream) for the catalysts at 723 K. For all the catalysts, the amount of CO is highest at the beginning and then decreases until it reaches some steady state value. This may be related to the rapid decrease in hydroxyl groups during the initial stages of the decomposition process. The largest CO content in the product stream was observed for ZSM-5 and the smallest for SiO<sub>2</sub>, which may be related to the amount/stability of the -OH groups present on the different supports. Figure 15 shows the rate of CO production during the

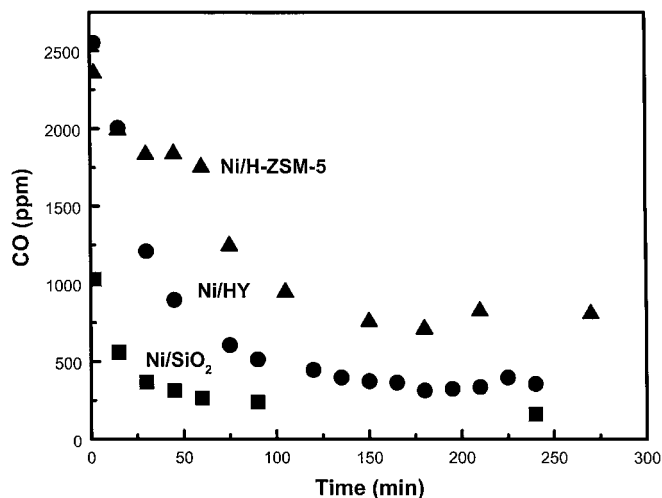


FIG. 14. CO content as a function of time for Ni supported on HZSM-5, HY, and SiO<sub>2</sub> at 723 K (GHSV = 20,000 cm<sup>3</sup> · g<sup>-1</sup> · h<sup>-1</sup>; 0.1 g of catalyst).

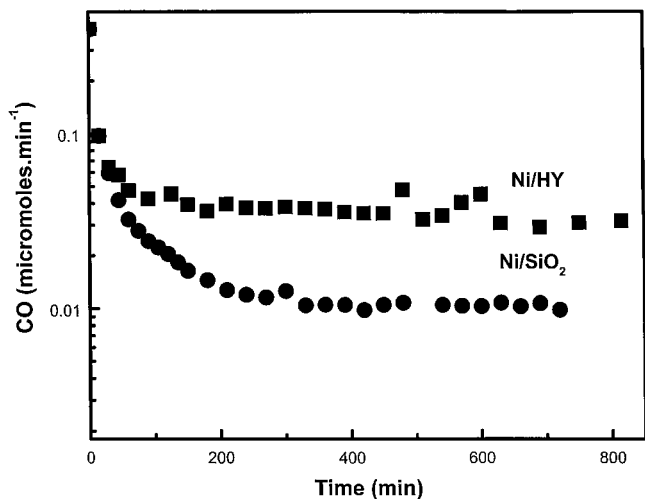


FIG. 15. Comparison of CO formation rates on Ni supported on HY and SiO<sub>2</sub> at 823 K (GHSV = 20,000 cm<sup>3</sup> · g<sup>-1</sup> · h<sup>-1</sup>; 0.1 g of catalyst).

methane decomposition on Ni/HY and Ni/SiO<sub>2</sub> at 823 K (GHSV = 20,000 cm<sup>3</sup> · h<sup>-1</sup> · g<sup>-1</sup>). The CO formation rates were similar initially for both catalysts, but with time decreased and stabilized to 0.01 and 0.035 μmol min<sup>-1</sup> for Ni/SiO<sub>2</sub> and Ni/HY, respectively. The total amount of CO formed (obtained by integrating the area under the curve) was found to be 14.5 and 29.4 μmol for Ni/SiO<sub>2</sub> and Ni/HY, respectively. DRIFTS experiments showed the presence of two types of hydroxyl species on silica; isolated and hydrogen bonded (similar to a previous study (28)). After the pretreatment of the catalyst and subsequent heating to 823 K, although the total hydroxyls were found to decrease a significant quantity was retained. The fraction of hydroxyl groups on silica remaining after heat treatment at various temperatures is well documented in literature (29–32). Previous studies showed that *in vacuo* heating of silica to 873 K resulted in elimination of approximately two-thirds of the initial hydroxyl groups (32). Considering the above and taking into account the hydroxyl density of un-pretreated silica and surface area of silica, calculations indicate the presence of approximately 55 μmol of hydroxyl species at 823 K on 0.1 g of Ni/SiO<sub>2</sub>. Occasionally ppm levels of CO<sub>2</sub> were observed in the product stream, but these were not accorded rigorous attention, as trace amounts of CO<sub>2</sub> do not pose significant problems to the PEM fuel cells. Therefore, it is difficult to estimate the fraction of the surface hydroxyl groups reacted in the process at this point. Further investigation will be required to quantitatively relate the hydroxyl groups to the CO<sub>x</sub> formed during the catalytic decomposition of methane.

## CONCLUSIONS

Methane decomposition on various Ni-supported catalysts revealed that there was a strong dependence of the

nature of the surface carbon and CO formation rates on the nature of the support. At high temperatures an encapsulating type of graphitic carbon was observed on Ni/H-ZSM-5 whereas Ni/HY and Ni/SiO<sub>2</sub> showed the presence of filamentous carbon, which resulted in a greater lifetime for the latter two and a very fast deactivation for the former. The carbidic form of carbon was present at low temperatures (≤723 K) but absent when higher temperatures were employed (>773 K) on all catalysts. The CO content in the hydrogen stream was found to be highest on Ni/H-ZSM-5 and lowest on Ni/SiO<sub>2</sub>. In general, CO formation rates were high initially but decreased rapidly with time and then remain steady until catalyst deactivation. The amount of CO in the hydrogen stream stabilized at ca. 250 ppm and 50 ppm for Ni/HY and Ni/SiO<sub>2</sub> at 823 K. Regeneration studies have shown that Ni/H-ZSM-5 retains its catalytic activity for methane decomposition over a number of reaction cycles at 723 K. Future studies addressing oxidative and steam regeneration are currently under way.

## ACKNOWLEDGMENTS

We acknowledge with pleasure the support of this work by the U.S. Department of Energy, Office of Basic Energy Sciences, Division of Chemical Sciences. We are grateful to Prof. Lunsford for kindly allowing us access to the DRIFTS setup. T.V.C. acknowledges the Link Foundation for the Link Energy Fellowship. C.C.C. gratefully acknowledges support from the Associated Western Universities, Inc., and Pacific Northwest National Laboratories operated by Battelle Memorial.

## REFERENCES

1. Rostrup-Nielsen, J. R., in "Catalytic Steam Reforming, Science and Engineering" (J. R. Anderson and M. Boudart, Eds.), Vol. 5. Springer, Berlin, 1984.
2. Rostrup-Nielsen, J. R., *Catal. Today* **18**, 305 (1993).
3. Choudhary, V. R., Mamman, A. S., and Sansare, S. D., *Angew. Chem., Int. Ed. Engl.* **31**, 1189 (1992).
4. Armor, J. N., *Appl. Catal.* **176**, 159 (1999).
5. Koerts, T., Deelan, M. J., and Van Santen, R. A., *J. Catal.* **138**, 101 (1992).
6. Koranne, M. M., and Goodman, D. W., *Catal. Lett.* **30**, 219 (1995).
7. Zadeh, J. M., and Smith, K. J., *J. Catal.* **183**, 232 (1999).
8. Belgued, M., Pareja, P., Amariglio, A., and Amariglio, H., *Nature* **352**, 789 (1991).
9. Beebe, T. P., Jr., Goodman, D. W., and Yates, J. T., Jr., *J. Chem. Phys.* **87**, 2305 (1987); Wu, M.-C., and Goodman, D. W., *Catal. Lett.* **24**, 23 (1994); Lenz-Solomon, P., Wu, M.-C., and Goodman, D. W., *Catal. Lett.* **25**, 75 (1994); Wu, M.-C., and Goodman, D. W., *Surf. Sci. Lett.* **306**, L529 (1994); Wu, M.-C., Xu, Q., and Goodman, D. W., *J. Phys. Chem.* **98**, 5104 (1994).
10. Choudhary, T. V., and Goodman, D. W., *J. Mol. Catal. A* **163**, 9 (2000).
11. Muradov, N. Z., *Energy Fuels* **12**, 41 (1998).
12. Zhang, T., and Amiridis, M. D., *Appl. Catal. A* **167**, 161 (1998).
13. Choudhary, T. V., and Goodman, D. W., *Catal. Lett.* **59**, 93 (1999).
14. Choudhary, T. V., and Goodman, D. W., *J. Catal.* **192**, 316 (2000).
15. Emrakova, M. A., Emrakov, D. Y., Plyasova, L. M., and Kuvshinov, G. G., *Catal. Lett.* **62**, 93 (1999).
16. Emrakova, M. A., Emrakov, D. Y., Kuvshinov, G. G., and Plyasova, L. M., *J. Catal.* **187**, 77 (1999).

17. Ferreira-Aparicio, P., Rodriguez-Ramos, I., and Guerrero-Ruiz, A., *Appl. Catal. A* **148**, 343 (1997).
18. Wagner, C. D., Riggs, W. M., Davis, L. E., Moulder, J. F., in "Handbook of X-ray Photoelectron Spectroscopy" (G. E. Muilenbuerg, Ed.). Perkin-Elmer Corp., Eden Prairie, MN, 1979.
19. Seah, M. P., *Surf. Interface Anal.* **14**, 488 (1989).
20. Barr, T. L., and Seal, S. J., *J. Vac. Sci. Technol. A* **13**, 1239 (1995).
21. Anderson, J. R., "Structure of Metallic Catalysts," p. 296. Academic Press, New York, 1975.
22. Rodriguez, N. M., *J. Mater. Res.* **8**, 3233 (1993).
23. Baker, R. T. K., Feates, F. S., Barber, M. A., Harris, P. S., and Waite, R. J., *J. Catal.* **26**, 51 (1972).
24. Rostrup-Nielsen, J. R., and Trimm, D. L., *J. Catal.* **48**, 155 (1977).
25. Mizokawa, Y., Nakanishi, S., Komoda, O., and Miyase, S., *J. Appl. Phys.* **67**, 264 (1990).
26. Belton, D. N., Harris, J. S., Schmiegel, S. J., Weiner, A. M., and Perry, T. A., *Appl. Phys. Lett.* **54**, 416 (1989).
27. Goodman, D. W., Kelley, R. D., Madey, T. E., and White, J. M., *J. Catal.* **64**, 479 (1980).
28. White, R. L., and Nair, A., *Appl. Spectrosc.* **44**, 69 (1990).
29. Fripiat, J. J., and Uytterhoeven, J., *J. Phys. Chem.* **66**, 800 (1962).
30. Taylor, J. A. G., and Hockey, J. A., *J. Phys. Chem.* **70**, 2169 (1966).
31. Zhuravlev, L. T., *Langmuir* **3**, 316 (1987).
32. Zhuravlev, L. T., *Colloids Surf. A: Physicochem. Eng. Aspects* **173**, 1 (2000).